

# Basin-scale migration of continental-rift brines: Paleohydrologic modeling of the Dead Sea basin

Eyal Stanislavsky  
Haim Gvirtzman } Institute of Earth Sciences, Hebrew University, Jerusalem 91904, Israel

## ABSTRACT

It was suggested that brine of the Dead Sea rift has originated from a residual product of intensively evaporated seawater that invaded the rift, precipitated halite, and later interacted through dolomitization with the host rock during subsurface migration. Detection of this brine in many deep wells located at distances as far as 100 km away from the rift was attributed to long-distance migration of the brine. The physical feasibility of such migration, which probably spanned the past 3–6 m.y., is quantitatively tested and verified in this study by using paleohydrologic modeling. The structural formation of the rift is described by a chronological sequence of geologic cross sections serving as the basis for hydrodynamic calculations, which assess the effects of the structure on fluid migration, salinity redistribution, and heat transport across the sedimentary basin. Results indicate that two basin-scale ground-water systems, one atop the other but with opposite flow directions, coexisted in the Dead Sea rift valley. The first is a topography-driven flow of meteoric water from the surrounding highlands toward the rift through relatively shallow aquifers ( $\leq 1$  km). The second is a density-driven migration of the Dead Sea brine through deep aquifers (4–5 km) in the opposite direction. The configuration of these flow systems has changed during the structural evolution of the Dead Sea rift, illustrating the interrelationships among basin formation, paleohydrology, and paleo geochemistry.

## INTRODUCTION

The Dead Sea rift (Fig. 1) is a left-lateral strike-slip transform, separating the Sinai-Levant subplate from the Arabian plate (Garfunkel and Ben-Avraham, 1996). The rift includes several en echelon rhomb-shaped grabens, one of which contains the Dead Sea and the lowest land-surface elevations on Earth (approximately –410 m). The Dead Sea basin evolved since 15 Ma. The basin fill has recorded three stages of evolution (Fig. 2, Table 1<sup>1</sup>). The continental conglomerate of the Hazeva Formation (unit Mh) represents the first stage, during which deposition kept pace with the rift subsidence. This regime ended in the late Miocene (8–10 Ma) when uplifting of the transform flanks and rapid subsidence of the basin led to a deep topographic trough. During the second stage, which began ~4–6 Ma, the basin was invaded by the Mediterranean Sea through the Yizre'el Valley (Fig. 1), forming an elongated seawater arm that evaporated, resulting in the deposition of the thick Sedom Formation evaporites (unit Qse). In the third stage, the basin was cut off from the open sea and became a closed basin. A hypersaline lake was formed, in which the fluviatile and lacustrine sediments of the Samra Formation (unit Qs) were deposited.

<sup>1</sup>GSA Data Repository item 9969, Figure S1, Map of deep boreholes, Table 1, Hydrostratigraphic units and their physical parameters, and Table 2, Brine's parameters at deep boreholes, is available on request from Documents Secretary, GSA, P.O. Box 9140, Boulder, CO 80301, [editing@geosociety.org](mailto:editing@geosociety.org), or at [www.geosociety.org/pubs/drpint.htm](http://www.geosociety.org/pubs/drpint.htm).

Starinsky (1974) analyzed ground-water samples from deep wells throughout Israel and defined two types of  $\text{CaCl}_2$  brines: coastal (C-type) and rift-related (R-type) ones (Table 2; see footnote 1). C-type brines are found mainly in wells along the Mediterranean coastal plain, whereas R-type brines occur mainly in the vicinity of the Dead Sea rift. The Na/Cl equivalent ratio of C-type brine is  $0.86 \pm 0.06$ , whereas that of R-type brine is significantly lower, reaching a minimum value of 0.15. The C-type brines are less saline than the R-type (120 and 400 g/L TDS [total dissolved solids], respectively). Starinsky (1974) first explained the geochemical evolution of these brines, and his explanation gained support from subsequent studies (e.g., Fleischer et al., 1977; Sass and Starinsky, 1979; Nativ, 1984). These studies suggest that the C-type brine is essentially slightly evaporated seawater in the range of gypsum precipitation, which is probably related to the Messinian episode. On the other hand, the R-type brine is a residual product of intensively evaporated seawater that invaded the Dead Sea rift, precipitated halite (e.g., the Sedom Formation), and later interacted with the host limestone (mainly dolomitization) during subsurface migration.

The spatial distribution of these brines is not well understood, especially because the R-type brines are found as far as 100 km away from the rift. Nor is it clear why the R-type brines are found mainly in deeper aquifers and the C-type brines occur in shallower ones. In wells where both brines are found, the R-type brine is located beneath the C-type one (Table 2 and Fig. S1; see

footnote 1). The argument of Starinsky (1974) that R-type brine originated within the rift and later migrated away through deep aquifers is based on geochemical interpretation. However, the physical feasibility of such long-distance migration, the forces involved, and the flow rate, duration, and pathways are unknown. In fact, one should expect an opposite flow direction because during rift-basin formation, topography-driven flow is the dominant flow mechanism, forcing ground water from the surrounding aquifers toward the deep drainage basin (Person and Garven, 1994). To date, little attention has been given to understanding the paleohydrology of the Dead Sea rift. This study attempts to fill this gap by presenting mathematical models that highlight the interrelationship between structural evolution and brine migration.

## PALEOHYDROLOGICAL MODELING

A detailed geologic cross section, 5 km deep by 170 km long, that traverses through the Mediterranean Sea, the Northern Negev, the Dead Sea, and the Moab Mountains (A–A' in Fig. 1) was prepared (Fig. 2A). The lithostratigraphic units involved, ranging in age from Cambrian to Quaternary, are listed in Table 1 (see footnote 1).

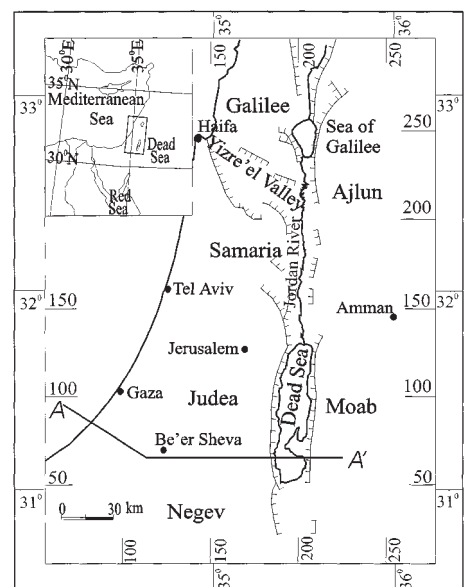
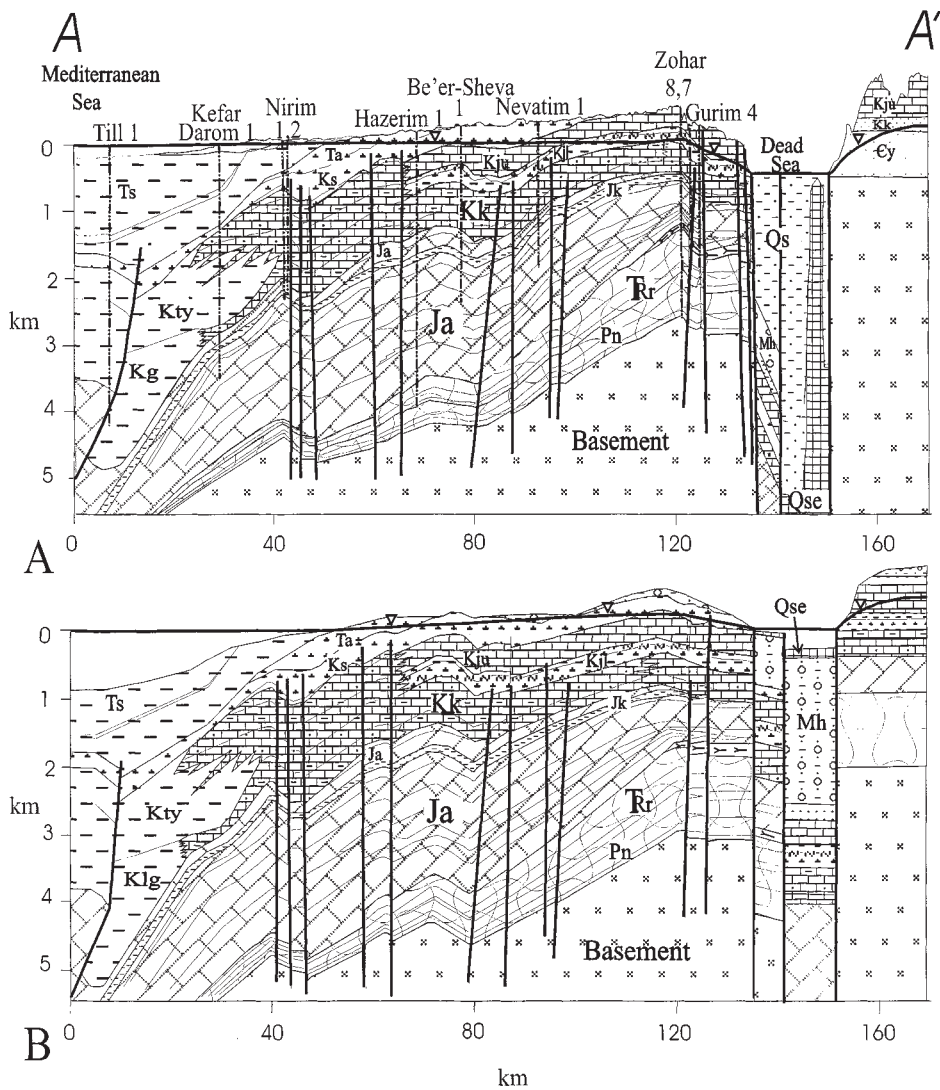


Figure 1. A map of studied area showing major faults along Dead Sea rift and location of geologic cross section A–A' (Fig. 2). Map coordinates refer to Israel grid system.

GSA Data Repository item 9969 contains additional material related to this article.



**Figure 2.** Evolution of the Dead-Sea rift (A–A', Fig. 1). **A:** Geologic cross section at present. **B:** Reconstructed geologic cross section for early Pliocene (about 3–6 Ma), when deposition of Sedom Formation started. Lithologic symbols are listed in Table 1 (see footnote 1). Formations were grouped into hydrostratigraphic units on the basis of their lithology and relative permeability.

The integrated stratigraphic sequence is grouped and divided into various hydrostratigraphic units according to their estimated hydraulic properties.

Mesozoic to Tertiary sediments crop out in the highlands on both sides of the rift valley and constitute the main recharge area for the major aquifers. Two regional aquifers contain most of the ground-water discharge to the rift: (1) the Upper Cretaceous Judea Group of predominantly platform carbonates (unit Kju); and (2) the Lower Cretaceous Kurnub Group of mainly continental sandstones (unit Kk). The subsiding rift valley is capped by a 10-km-thick Miocene–Quaternary sequence consisting of alluvial deposits and evaporites, which are mostly aquitards. The ground-water systems on both sides of the rift have become separated because of juxtaposition of aquifers on the flanks with aquitards across the faults in the rift valley (Gvirtzman et al., 1997a, 1997b).

Another geologic cross section was constructed along the same line (Fig. 2B) for the time when deposition of the Sedom Formation had begun and the R-type brine had originated. An important assumption is that the sea, which invaded the rift valley during the deposition of the Sedom Formation, was connected to the Mediterranean Sea and had the same elevation. Subsequently, the lake level has gradually dropped at an assumed constant rate.

Our approach was to adopt the deformed section as the basis for the hydrodynamic calculations to assess the effects of the structure on fluid migration, salinity redistribution, and heat transport across the sedimentary basin (Fig. 3). Computations were conducted through the use of the JHU2D code (Garven and Freeze, 1984). This two-dimensional code uses the finite-element method to solve the transient fluid and heat-flow equations. The simulated domain includes the

sedimentary sequence between the ground-water table (top boundary) and the basement (bottom boundary). Assignment of material properties (Table 1; see footnote 1) for each of the hydrostratigraphic units is based on estimates derived from literature compilations and sensitivity analyses. Longitudinal and transverse dispersivities of 200 m and 20 m, respectively, were chosen for all hydrostratigraphic units which are reasonable for the scale involved (Gelhar et al., 1992). Simulations were conducted for both time periods (3 or 6 Ma) because of the uncertainty regarding the age of the Sedom Formation, which is equal to the age of R-type brine and to its migration period (Garfunkel and Ben-Avraham, 1996).

Hydraulic boundary conditions are defined by atmospheric pressure at the ground-water table. At the base of the cross section and at its western and eastern sides, no-flow boundary conditions are assumed (Gvirtzman et al., 1997a). Thermal boundary conditions are defined with a constant temperature of 20 °C at the water table, as suggested by a Mediterranean climate. A steady geothermal flux of 45 mW/m<sup>2</sup> is assumed at the bottom boundary (Eckstein and Simmons, 1978). Insulated boundaries have been assumed at both sides of the cross section. Boundary conditions of water salinity (grams of NaCl per 1 g H<sub>2</sub>O) were assumed to be 0.0005 g/g at most of the top boundary, where rainwater infiltrates through the land surface, 0.267 g/g at the Dead Sea, and 0.034 g/g at the Mediterranean Sea (Fig. 3A). Initial conditions are assumed to be equal to seawater salinity (0.034 g/g) throughout the cross section, but 0.098 g/g (typical for deposition of gypsum) is assumed in a small domain beneath the Mediterranean Sea, reflecting the C-type brine that originated during the Messinian episode (Starinsky, 1974).

## SIMULATION RESULTS

Flow directions and salinity redistribution throughout the section at five sequential stages of basin evolution are shown in Figure 3. These numerical simulations assume that the brine originated 3 Ma (Fig. 3A). Once the seawater within the rift partially evaporated and became more saline, conditions became unstable, with this heavier water overlying lighter ground-water. Thus, water penetrated rapidly downward (Fig. 3B). While sinking, at least two small density-driven free-convection cells (counterclockwise and clockwise) were initiated within the faulting blocks, having vertical-flow velocities of about 10 m/yr. At the same time, formation water within a significant part of the sedimentary sequence at the rift flanks was displaced westward, with flow rates of 0.1 m/yr at most.

Subsequently, a secondary unstable condition along the horizontal plane became dominant. The equivalent-fresh-water head of ground water at a depth of 4 km within the basin fill was calculated to be about 700 m, higher than that in the rift

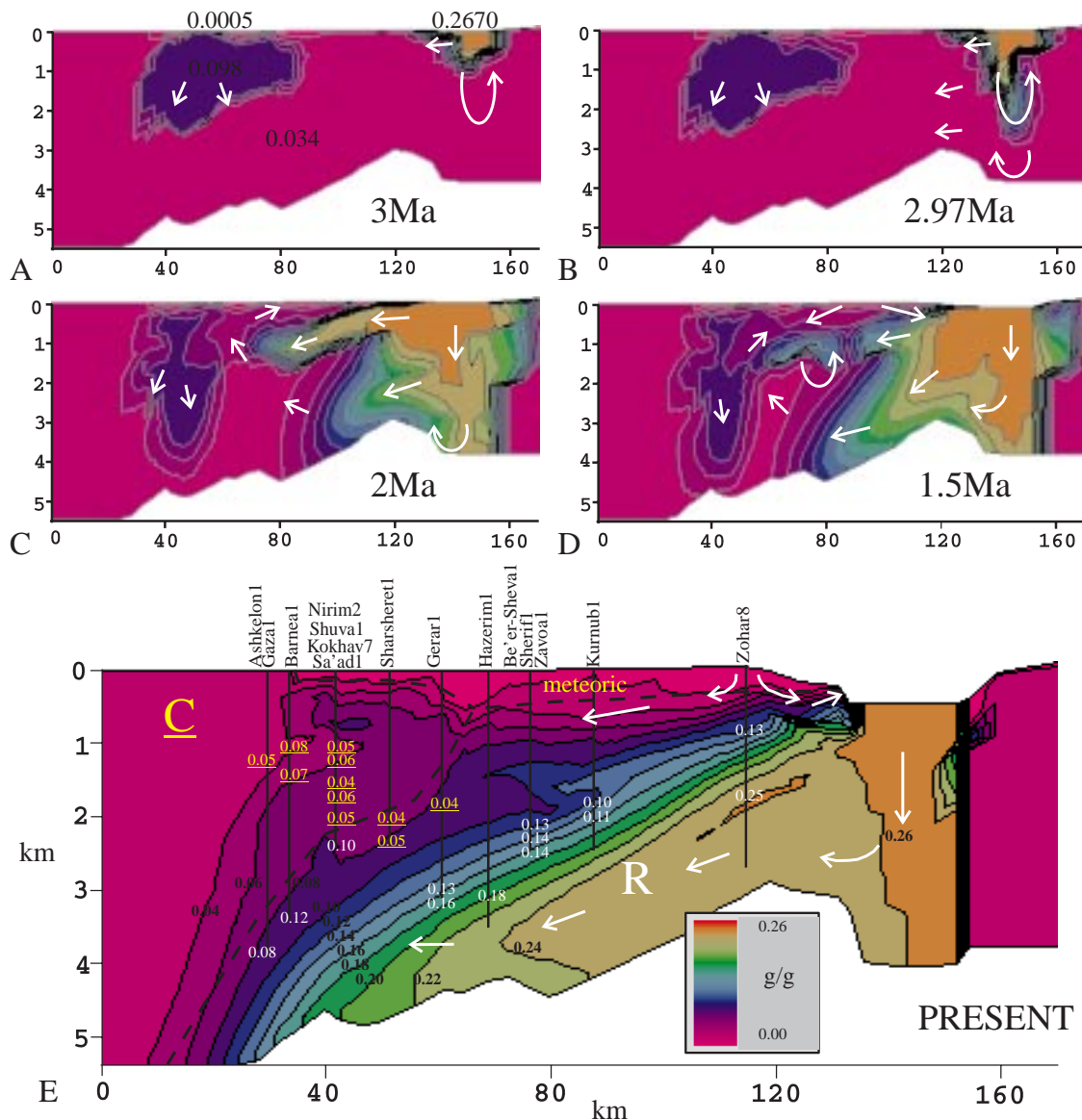


**Figure 3.** Numerical simulations of salinity redistribution and schematic ground-water flow directions at five sequential stages during structural evolution of Dead Sea rift (since 3 Ma), demonstrating migration of rift-type brine. **A:** Residual product of intensely evaporated seawater first introduced into rift valley. Large salinity cloud on west side is C-type brine, which is related to the Messinian episode. **B:** Penetration of heavy, saline, evaporated water into basin fill. **C:** Lateral brine migration into upper aquifer. **D:** Mixing and dilution of front moving brine at upper aquifer and slow lateral migration into lower aquifers. **E:** Present salinity distribution, created by continuous lateral brine migration into lower aquifers and “flushing” of previously intruded brine toward rift by topography-driven flow at upper aquifer. Favorable matching was obtained between calculated isosalinity contours and measured (Table 2; see footnote 1) ground-water salinity in boreholes (white numbers for R-type and underlined yellow numbers for C-type brines). Dashed black line borders describe estimated distribution of ground-water bodies.

flanks. This initiated a density-driven lateral migration of brine from the basin fill westward. Lateral migration occurred either in deep or in shallow layers, depending on their relative hydraulic permeability. Because hydraulic conductivities of the Cretaceous aquifers are higher than those of the Jurassic and Triassic ones, brine migration started in the upper layer (Fig. 3C). As a result, vertical unstable conditions formed again, inducing free-convection cells within the Cretaceous aquifers, which resulted in mixing and dilution of the front moving brine (Fig. 3D). Brine migration was channeled only into the sedimentary sequence because of the low permeability of the basement. The thickness of the sedimentary sequence at the eastern side of the rift changed during the simulated period because of the lateral shift along the transform and the differential uplift at both its sides (Fig. 2).

Once the basin was cut off from the open sea and the lake level dropped, notable hydraulic

gradients between the surrounding highlands and the rift valley were formed, inducing local topography-driven flows toward the drainage basin, mainly through shallow aquifers. As levels of the rift's lake lowered, the hydraulic gradients became steeper. The topography-driven flow systems became more forceful with linear velocities of a maximum of 20 m/yr affecting larger adjacent areas and inducing deeper-reaching flow-lines. Consequently, a “flushing” mechanism was initiated with a reversed flow direction, in which the percolating meteoric water at the highlands displaced the previously intruded brine back into the rift (Fig. 3D, E). Along the rift margins, new springs emerged, discharging a mixture of cold, fresh ground water from shallow aquifers (down to 0.5 km) and ancient warm brine from deep ones (down to about 1 km). At the same time, at much deeper horizons (1–4 km), flow continued in the opposite direction, forcing the brine westward into the Jurassic and Triassic aquifers. Cal-

culations show that westward brine migration still occurs today at rates of ~0.05 m/yr.

Lateral brine migration took place at different horizons during the geologic history not only because of the deepening of the topography-driven flow system, but also because of the plumbing effect—the direct effect of basin configuration. As faulting of permeable units proceeded within the rift valley, adjacent aquifers at the rift flanks were being truncated or connected, changing the available pathways for ground-water flow (Wieck et al., 1995). The most permeable unit of the sedimentary fill is the Hazeva Formation conglomerate. The heavy saline seawater (or, later, lake water) at the rift valley sunk downward, mostly through the Hazeva Formation (or through open fractures), and moved laterally into the adjacent aquifers. Therefore, as the Hazeva Formation subsided (Fig. 2), saline water was transferred into deeper aquifers at the basin's flanks, first into the Creta-

ceous aquifers, then into the Jurassic, and finally into the Triassic and Permian ones.

At the first stage, during westward brine intrusion, the total masses of salt that entered the Cretaceous Judea and Kurnub aquifers were  $2.3 \times 10^{11}$  and  $4.4 \times 10^9$  kg per 1-m-width slice of cross section, respectively. At the second stage, during flushing of the brine back to the rift, salt masses that left these aquifers were  $1.9 \times 10^{11}$  and  $3.7 \times 10^9$  kg per 1-m-width slice of cross section, respectively. In other words, more than 80% of the invading brine has subsequently been washed back into the Dead Sea. At the deeper Jurassic and Triassic aquifers, during both stages,  $2.6 \times 10^{10}$  kg of salt per 1-m-width slice of cross section has intruded westward.

Sensitivity of the modeling results was explored by varying hydraulic parameters until the comparison between calculated and measured ones seemed favorable. Measured data of current ground-water recharge and discharge, geothermal gradients, salinities, and brine types were used for the adjustment of the various hydrostratigraphic properties. Assignment of 0.1 and 0.2 m/yr as horizontal hydraulic conductivity for the Jurassic and Triassic sediments has produced sufficient fitting for migration periods of 6 and 3 Ma, respectively. Nevertheless, the best simulation results were those assuming brine migration to have taken place since 3 Ma (Fig. 3).

## DISCUSSION

Absolute hydraulic and thermal parameters cannot be proved, verified, or validated by such numerical models as ours, because of the many assumptions and simplifications that have been made (Oreskes et al., 1994). For example, these modeling experiments have not accounted for changes of fluid-density or rock permeability due to water-rock interactions while water is migrating through aquifers (e.g., dolomitization). Similarly, we neglected compaction-driven and tectonically driven flow systems and effects of climate fluctuations. Nevertheless, these numerical experiments consider the dominant processes and therefore provide a first-order understanding of ground-water system behavior and furnish reasonable ranges of material property values.

Our hypothesis provides insight into the geochemical composition of the Dead Sea water. Starinsky (1974) argued that according to geochemical trends, the current Dead Sea water does not represent a pure residual product of intensively evaporated seawater. Rather, it is a brine that has interacted subsequently with the surrounding rocks, mainly via dolomitization. The physical mechanisms of migrating into the surrounding rocks and later back into the lake remained unclear. Our suggested mechanisms of

the density-driven ground-water flow and the subsequent flushing mechanism support Starinsky's hypothesis. Furthermore, the total masses of salts, which were flushed from the Cretaceous aquifers back into the rift's lake, are an order of magnitude larger than the salt mass currently dissolved in the Dead Sea. Therefore, the geochemical composition of the lake water is R-type brine.

Person and Garven (1994) argued that during the initial stages of continental-rift-basin formation, topography-driven flow is the most dominant mechanism because of the steep slopes in the ground-water table associated with the formation of narrow fault-bounded troughs. In this study, however, we describe and quantitatively reconstruct a basin-scale (across 100 km) density-driven ground-water migration, which, surprisingly, takes place during the initial rifting phase of a continental rift. Generalization of this mechanism to any closed, deep, and arid continental rift basin seems feasible, but needs further investigation.

## CONCLUSIONS

Buoyancy-driven flow associated with salinity variations is proposed as the principal driving force that has caused the migration of brine from the Dead Sea to a distance ~100 km to the west through deep aquifers. Numerical simulations indicate the coexistence of two basin-scale ground-water flow systems, one atop the other with opposite flow directions. The first is a topography-driven ground-water flow from the surrounding highlands toward the rift valley through relatively shallow aquifers ( $\leq 1$  km). The second is a density-driven migration of brine through deeper aquifers (4–5 km) in the opposite direction, from the rift outward. The configuration of the two flow systems changed during basin formation; both were deepening with time. Therefore, in the intermediate horizon, the invading brine was later flushed, which is reflected in the lake's chemical composition. Salinity distribution is still far from steady-state conditions and thus, brine still migrates from the Dead Sea basin westward through the deep Jurassic and Triassic formations.

## ACKNOWLEDGMENTS

We thank A. Starinsky and Y. Kolodny for their insightful remarks and V. Lyakhovsky for his help with the modeling. This research is a part of Stanislavsky's M.Sc. thesis. The research was supported by a grant from the Water Commission of Israel.

## REFERENCES CITED

- Eckstein, Y., and Simmons, G., 1978, Measurements and interpretation of terrestrial heat flow in Israel: *Geothermics*, v. 6, p. 117–142.
- Fleischer, L., Goldberg, M., Gat, J. R., and Magaritz, M., 1977, Isotopic composition of formation waters from deep drilling in southern Israel: *Geochimica et Cosmochimica Acta*, v. 41, p. 511–525.
- Garfunkel, Z., and Ben-Avraham, Z., 1996, The structure of the Dead Sea Basin: *Tectonophysics*, v. 266, p. 155–176.
- Garven, G., and Freeze, R. A., 1984, Theoretical analysis of the role of groundwater flow in the genesis of stratabound ore deposits: 2. Quantitative results: *American Journal of Science*, v. 284, p. 1125–1174.
- Gelhar, L. W., Welty, C., and Regfeldt, R. K., 1992, A critical review data on field-scale dispersion in aquifers: *Water Resources Research*, v. 28, p. 1955–1974.
- Gvirtzman, H., Garven, G., and Gvirtzman, G., 1997a, Thermal anomalies associated with forced and free ground-water convection in the Dead Sea Rift Valley: *Geological Society of America Bulletin*, v. 109, p. 1167–1176.
- Gvirtzman, H., Garven, G., and Gvirtzman, G., 1997b, Hydrogeological modeling of the saline-hot springs at the Sea of Galilee, Israel: *Water Resources Research*, v. 33, p. 913–926.
- Nativ, R., 1984, The water potential of the deep Jurassic to Paleozoic aquifers in the Negev, Israel. [Ph.D. thesis]: Be'er-Sheva, Israel, Ben-Gurion University, 311 p. (in Hebrew).
- Oreskes, N., Shrader-Frechette, K., and Belitz, K., 1994, Verification, validation and confirmation of numerical models in the earth sciences: *Science*, v. 263, p. 641–646.
- Person, M., and Garven, G., 1994, A sensitivity study of the driving forces on fluid flow during continental-rift basin evolution: *Geological Society of America Bulletin*, v. 106, p. 461–475.
- Sass, E., and Starinsky, A., 1979, Behavior of strontium in subsurface calcium chloride brines: Southern Israel and Dead Sea rift valley: *Geochimica et Cosmochimica Acta*, v. 43, p. 885–895.
- Starinsky, A., 1974, Relationship between Ca-chloride brines and sedimentary rocks in Israel [Ph.D. thesis]: Jerusalem, Israel, Hebrew University, 176 p. (in Hebrew).
- Wieck, J., Person, M., and Strayer, L., 1995, A finite element for simulating fault block hydrothermal fluid flow within rifting basins: *Water Resources Research*, v. 31, p. 3241–3258.

Manuscript received March 4, 1999

Revised manuscript received May 25, 1999

Manuscript accepted June 2, 1999